

Supplementary Information

Interfacial degradation mechanism in inverted perovskite solar cells with sol-gel derived NiO_x hole transport layer

Abraha Tadesse Gidey,^{a,b,c,*} Elias Assayehegn,^c Esayas Alemayehu,^d Alexander R. Uhl,^b and
Jung Yong Kim^{e,f,*}

^a Faculty of Materials Science and Engineering, Jimma Institute of Technology, Jimma University, Jimma P.O. Box 378, Ethiopia

^b Laboratory for Solar Energy and Fuels (LSEF), School of Engineering, The University of British Columbia, Kelowna V1V1V7, Canada

^c Department of Chemistry, College of Natural and Computational Sciences, Mekelle University, Mekelle P.O. Box 231, Ethiopia

^d Faculty of Civil and Environmental Engineering, Jimma Institute of Technology, Jimma University, Jimma P.O. Box 378, Ethiopia

^e Department of Materials Science and Engineering, Adama Science and Technology University, Adama P.O. Box 1888, Ethiopia

^f Center of Advanced Materials Science and Engineering, Adama Science and Technology University, Adama P.O. Box 1888, Ethiopia

* Correspondence:

Abraha.tadesse@mu.edu.et (A.T.G.)

jungyong.kim@astu.edu.et (J.Y.K.)

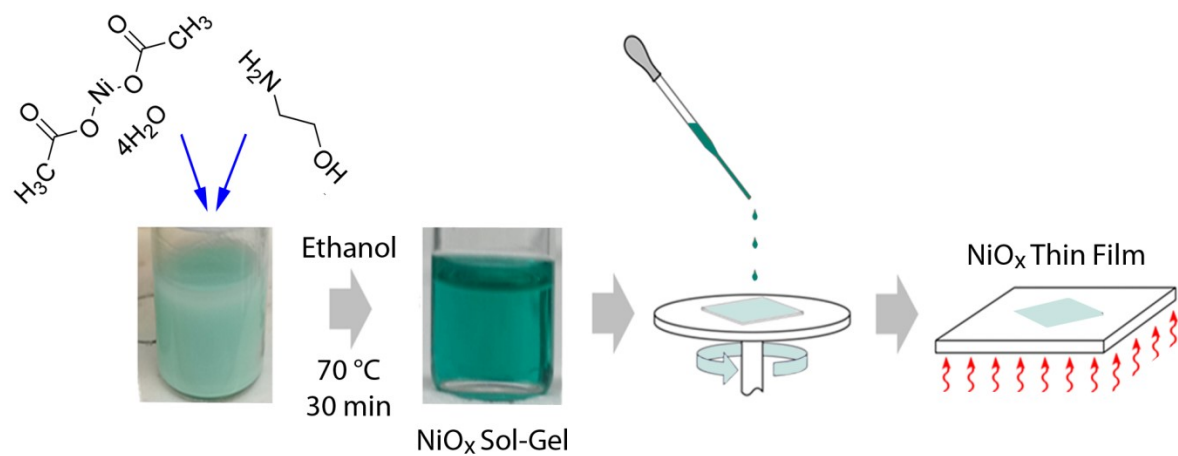


Figure S1. Synthesis pathway of NiO_x sol-gel and thin films

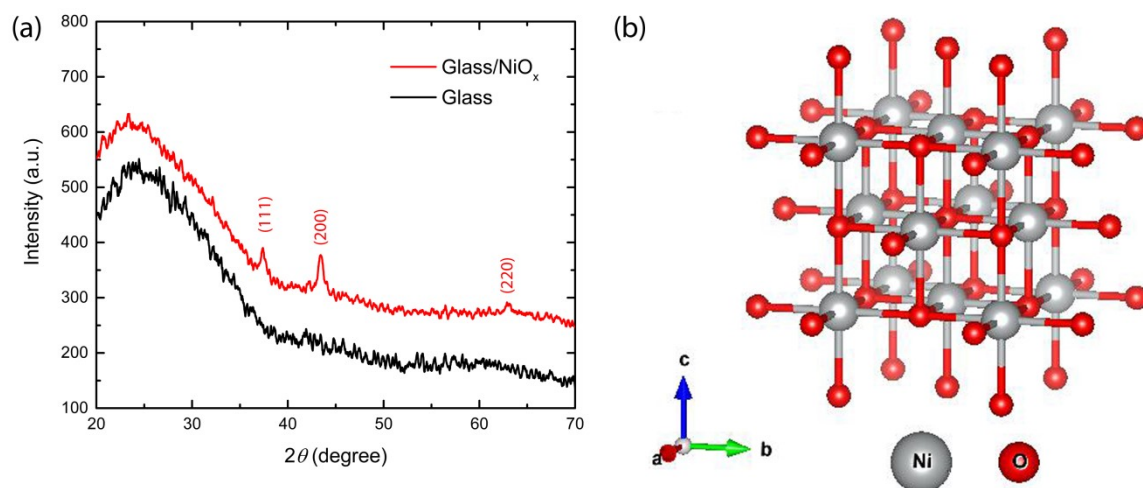


Figure S2. (a) XRD patterns of NiO_x thin films deposited on the glass substrate and (b) unit cell of NiO displaying face-centered cubic (FCC) structure.

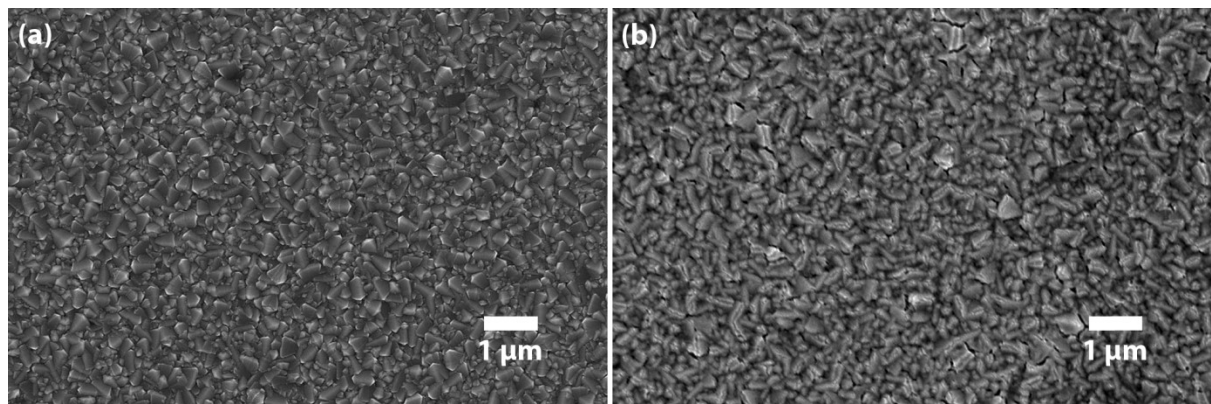


Figure S3. Top SEM images (a) bare FTO and (b) NiO_x

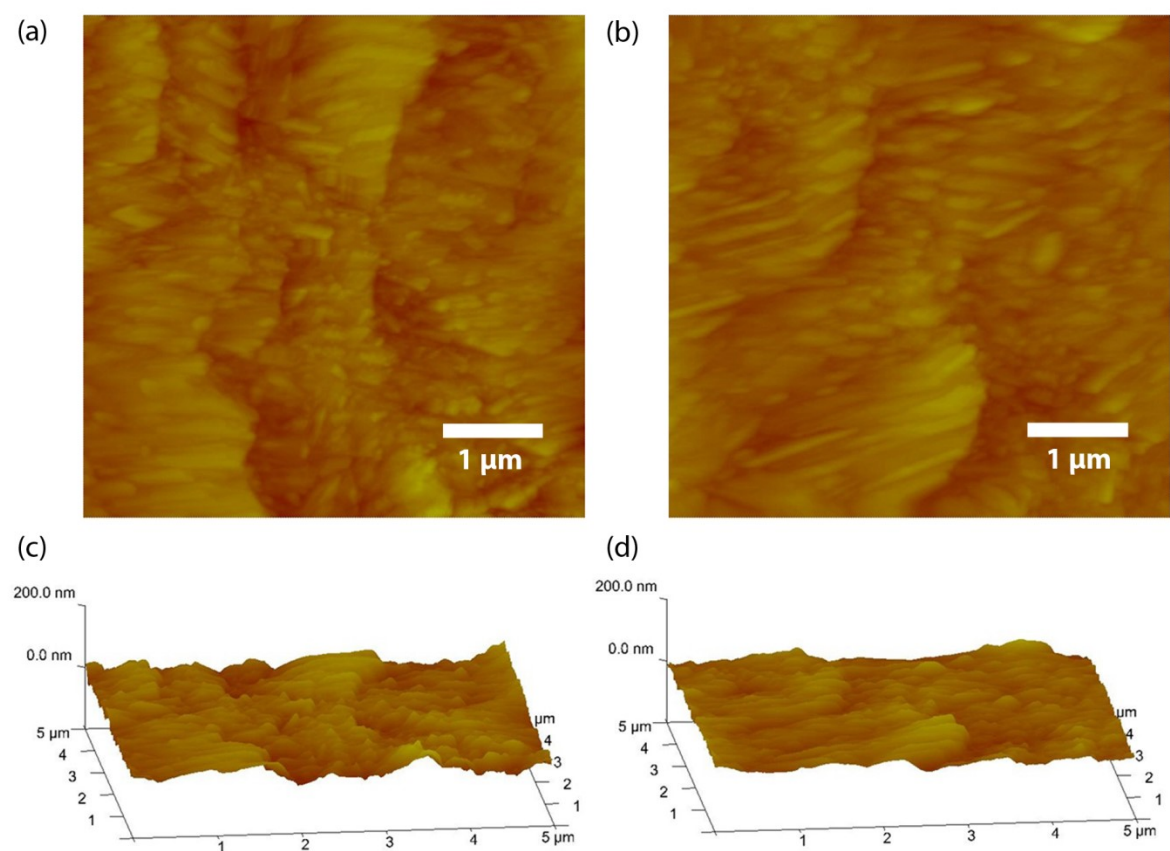


Figure S4. Top AFM images of: (a) bare FTO, (b) NiO_x deposited on FTO, (c) 3D AFM images bare FTO, and (d) 3D AFM image of NiO_x deposited on FTO.

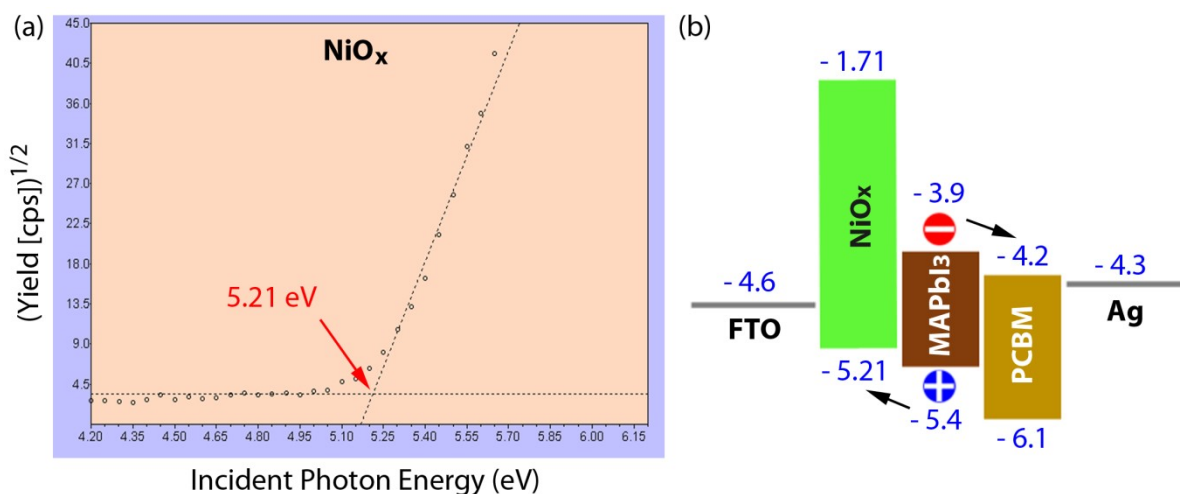


Figure S5. (a) Work function of NiO_x , (b) Energy levels of each layer used in inverted MAPbI₃-based PSCs.

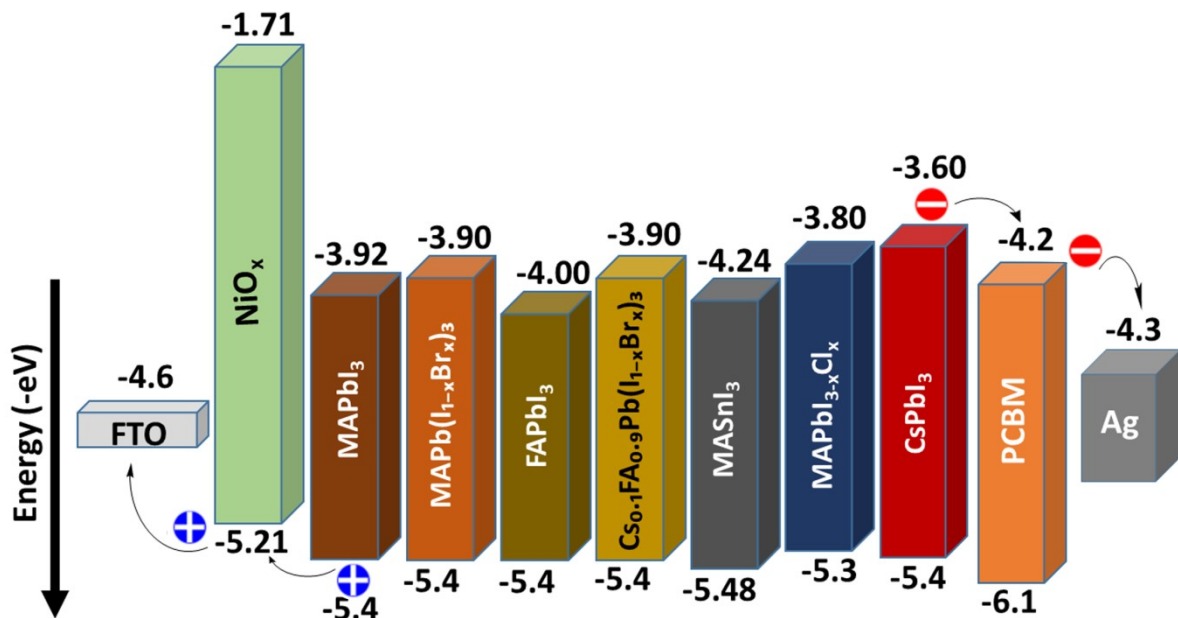


Figure S6. Energy-level diagram showing the valence band (VB) and conduction band (CB) positions of various common perovskites.

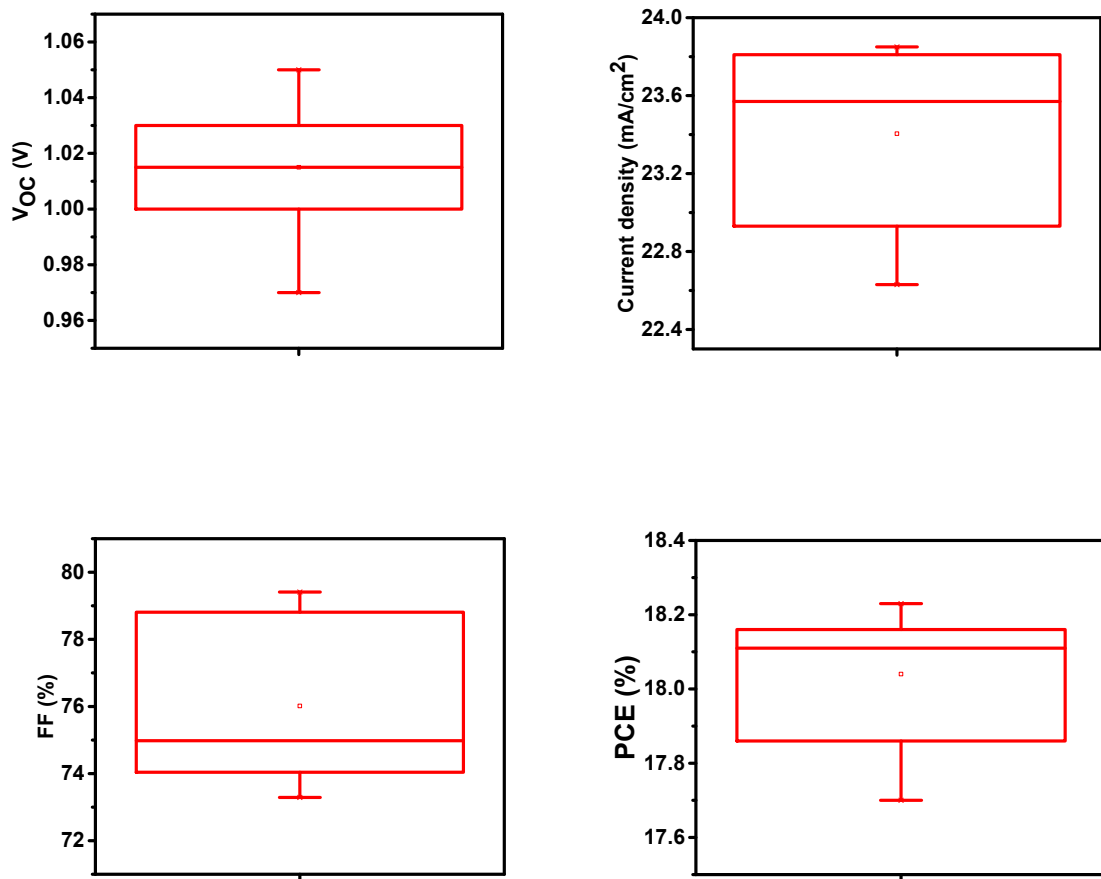


Figure S7. Statistical box plots of the PV parameters: (a) V_{OC} , (b) J_{SC} , (c) FF, and (d) PCE, obtained from MAPbI_3 -based fresh devices using NiO_x as HTL.

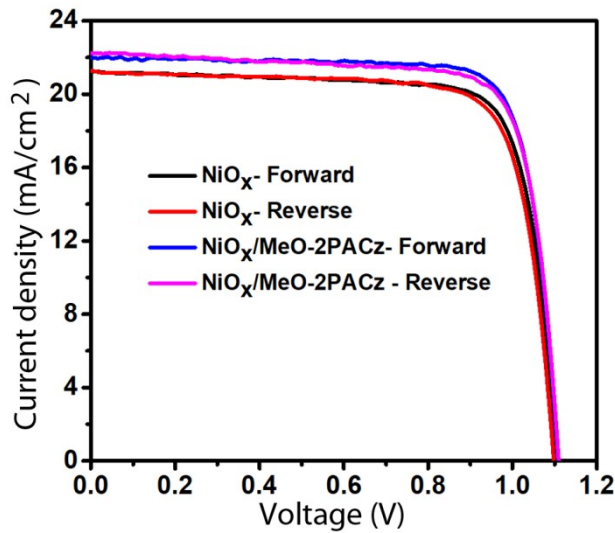


Figure S8. J - V of the champion CsFAMA-based perovskite solar cells.

Table S1. Photovoltaic performances of the NiO_x -based inverted perovskite solar cells. The statistics are based on 10 devices.

Device Structure	V_{OC} (V)	J_{SC} (mA/cm^2)	FF (%)	PCE (%)
FTO/ $\text{NiO}_x/\text{MAPbI}_3/\text{PCBM/Ag}$	1.02 ± 0.03	23.40 ± 0.48	76.01 ± 2.52	18.04 ± 0.18
FTO/ $\text{NiO}_x/\text{CsFAMAPbI}_3/\text{PCBM/Ag}$	1.06 ± 0.41	21.69 ± 0.60	78.05 ± 1.90	17.99 ± 0.22
FTO/ $\text{NiO}_x/\text{MeO-2PACz/}$ $\text{CsFAMAPbI}_3/\text{PCBM/Ag}$	1.08 ± 0.34	22.37 ± 0.52	79.56 ± 1.36	19.13 ± 0.34